

# MODELLING THE EXTRACTION OF SUGAR FROM SUGAR CANE IN A DIFFUSER

C. Breward\*, G. Hocking<sup>†</sup>, H. Ockendon<sup>‡</sup>, C. Please<sup>§</sup>  
and D. Schwendeman<sup>¶</sup>

## Study group participants

A. Adolinline, C. Breward, R. Ferdinand, B. Florio, N. Fowkes,  
G. Hocking, A. Hutchinson, M. Khalique, D.P. Mason, H. Ockendon,  
C. Please and M. Rademeyer

## Industry representatives

Richard Loubser and Steve Davis

## Abstract

Discrete and continuous mathematical models are constructed for the flow of sugarcane and juice through a sugar diffuser. The models describe how the concentration of sugar in the juice increases during the process. The flow through the sugar cane in the diffuser is analysed. It is found that the fluid moves downwards with constant velocity. The injection of tracer on one of the jets is modelled. The diffusivity of the tracer is different for the direction of flow and across the flow. The model is able to reproduce the behaviour observed in tracer experiments. A cavitation mechanism is investigated for creating dry regions in voids in the sugar cane. It is shown that the voids occur when the

---

\*Oxford Centre for Collaborative Applied Mathematics, University of Oxford, Oxford, United Kingdom, *email: breward@maths.ox.ac.uk*

<sup>†</sup>School of Chemical and Mathematical Sciences, Murdoch University, Perth, Western Australia, Australia, *email: g.hocking@murdoch.edu.au*

<sup>‡</sup>Oxford Center for Industrial and Applied Mathematics, University of Oxford, Oxford, United Kingdom, *email: ockendon@maths.ox.ac.uk*

<sup>§</sup>Oxford Centre for Collaborative Applied Mathematics, University of Oxford, Oxford, United Kingdom, *email: please@maths.ox.ac.uk*

<sup>¶</sup>Oxford Centre for Collaborative Applied Mathematics, University of Oxford, Oxford, United Kingdom, *email: scgwed@rpe.edu*

permeability varies with depth in a way to produce regions of negative pressure. Their existence depends on the variation in the permeability through the whole depth but especially on regions of low permeability away from the bottom of the bed.

## 1 Introduction

This problem is about the process of extracting sugar from shredded sugar cane using a device known as a diffuser, as shown in Figure 1. Shredded sugar cane is fed into one end of the diffuser and travels down a conveyor belt to the other end, where it is then passed through a set of rollers. The sugar cane in the diffuser is known as megasse. “Fresh” water is introduced from above at the opposite end of the diffuser, passes through the cane and gets collected in a tray underneath the conveyor belt. As the water passes through the cane, some of the sugar dissolves into the water, turning it into “juice”. The transfer rate depends on the difference in concentration between the sugar in the cane and the sugar dissolved in the water. Once the juice has been collected beneath the conveyor belt, it is pumped around and reintroduced upstream, passes through the cane and is collected again. This process is repeated around twelve times (the exact number depending on which diffuser is used), by which time the juice has reached the upstream end of the diffuser, after which it is collected and sent to the factory for processing. The process is continuous and 100

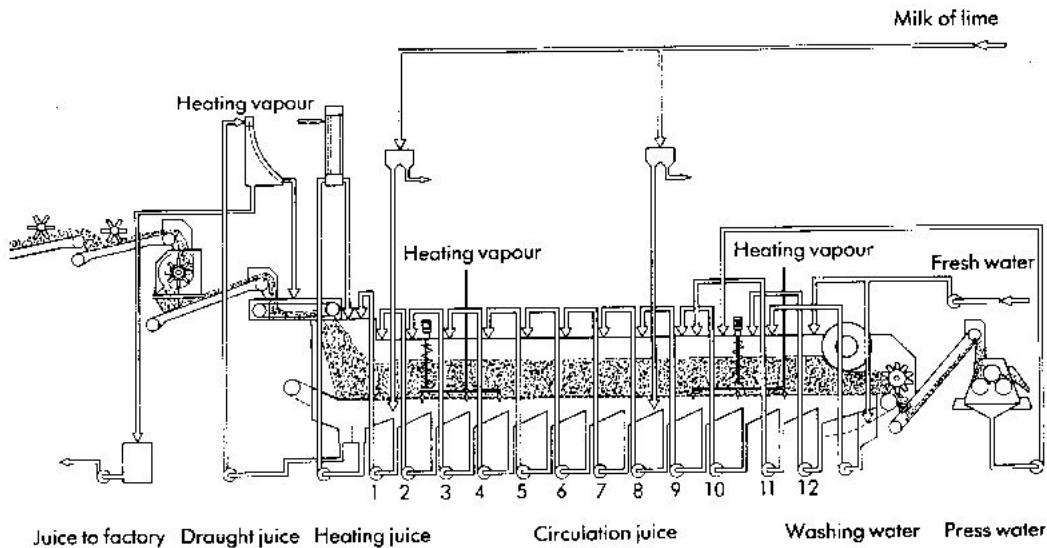


Figure 1: Schematic showing the diffuser.

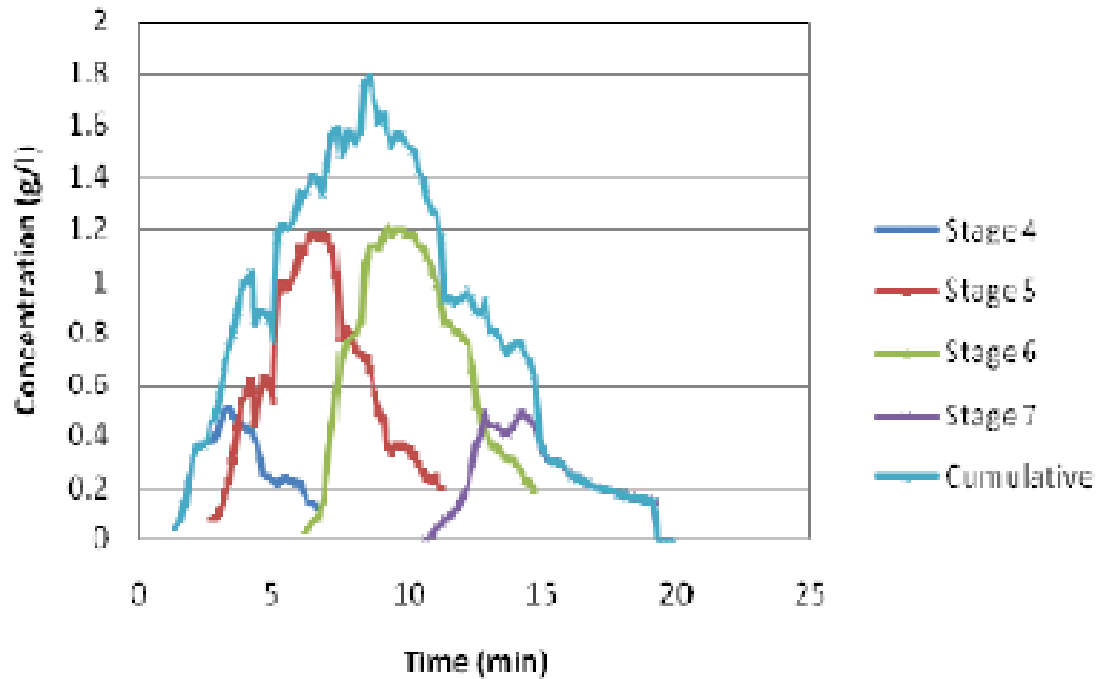


Figure 2: Tracer experiments

tonnes of sugar cane are processed each hour.

Experiments have been carried out in which a tracer is introduced into the juice at one specific inlet, and the concentration in the trays monitored. The results show that the tracer appears in five trays, as shown in Figure 2. It is believed that this spreading leads to inefficiencies in the device. Other experiments are carried out using a column.

### 1.1 Some experimental parameters and observations

Dry shredded cane comprises a fibre portion, containing slender pieces 25 – 100 mm long, and 1 – 5 mm thick, and fine material made up from pith and short fibres, as shown in Figure 3. The fibre component forms around 70% of the cane by dry mass. The fine material tends to accumulate at the bottom of the megasse. Of the 100 tonnes per hour of cane supplied at the inlet to the diffuser, 70 tonnes is bound water, 15 tonnes is fibre and 15 tonnes is sugar. It is observed that air-filled voids can form within the megasse and these are thought to be undesirable.

A typical diffuser has length 60m with 12 – 14 stages, a width of 4m, a wet bed



Figure 3: Shredded cane

height of 1.8m and a conveyor belt velocity of 0.8m/min. The flux of material along the conveyor belt,  $Q_h = 0.8 \times 1.8 \times 4 = 5.8\text{m}^3/\text{hr}$ . The flux of water supplied to the diffuser is adjusted so that the bed is almost completely saturated but that liquid from one inlet is kept distinct from the liquid from its neighbours. This can result in some localised surface flooding.

## 1.2 Key questions

The key questions to be addressed are:

- Are “column experiments” any good for simulating the diffuser?
- What cane characteristics are desired for optimal sugar extraction? In particular, what is the effect of having voids in the megasse?
- What can be done to achieve plug flow beneath the inlets?

## 1.3 Water balance

Before we turn to making a model for the operation of the diffuser, we consider the overall water balance in the process, including the water bound within the fibrous bed. This is shown diagrammatically in Figure 4. As stated in Section 1.1, the 100 tonnes/hr of shredded cane entering the diffuser contains 70 tonnes/hr of bound water. As the cane passes under the the first jet, the bound water content increases to 85 tonnes/hr. Clean water is supplied above the end of the conveyor belt at a rate of 50 tonnes/hr. The megasse leaving the conveyor belt contains the 85 tonnes/hr

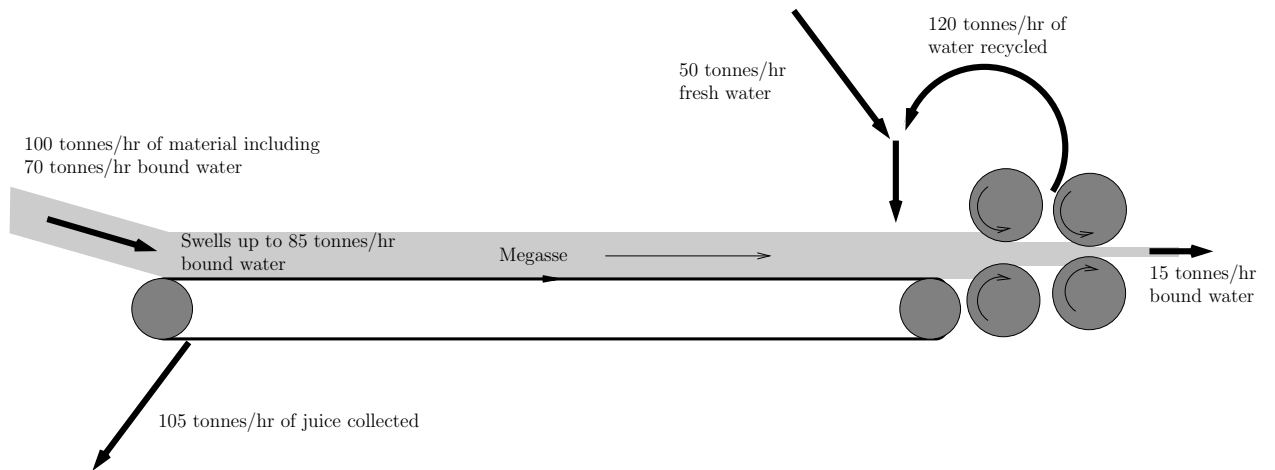


Figure 4: Schematic showing water balance in the diffuser.

of bound water and 50 tonnes/hr of free water. It is passed through two sets of rollers, resulting in a bed containing 15 tonnes/hr of bound water and 15 tonnes/hr of fibre. The 120 tonnes/hr of water squeezed out by the rollers is reintroduced into the system at the same point as the clean water. Finally, 105 tonnes per hour of juice is removed from beneath the start of the diffuser.

#### 1.4 Forward look

In Section 2 of this report we will generate and solve several simple mathematical models for the evolving concentration of sucrose in the diffuser. In Section 3 we will examine the flow of juice through the megasse in order to try and explain the tracer experiments. Finally, in Section 4 we will look at mechanisms for the formation of voids.

## 2 Models for the sucrose concentration in the diffuser

In this section we will formulate and solve simple discrete and continuous models for the concentration in the diffuser, ignoring the results of the tracer experiments which indicate that there is significant spread of liquid as it falls through the megasse.

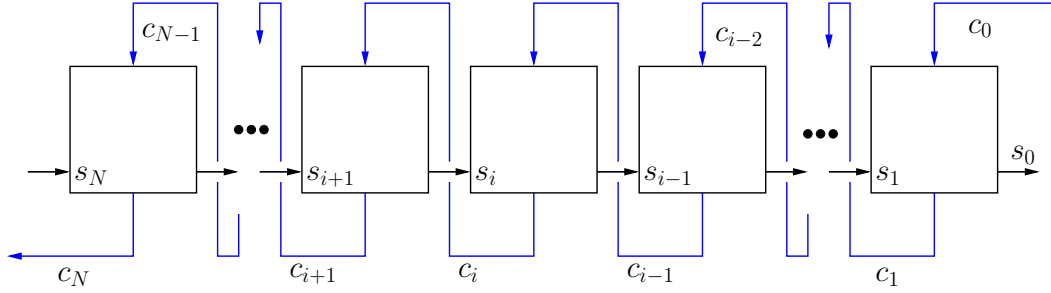


Figure 5: Schematic diagram of the discrete model.

## 2.1 Discrete model

The simplest discrete model is a compartmental model as illustrated in Figure 5.<sup>1</sup> We use this model to track the sucrose concentration  $C$  in the juice, and  $S$  in the shredded cane. We measure concentrations in tonnes/m<sup>3</sup>. Each compartment has height  $h$ , width  $l$  and depth  $d$  (perpendicular to the plane of the diagram). The  $i$ -th compartment is supplied with a volume flux  $Q_v$  of juice with sucrose concentration  $C_{i-1}$  from the compartment on the right and a volume flux  $Q_h$  of megasse with sucrose concentration  $S_i$  from the compartment on the left. We relate the fluxes to the horizontal and vertical velocities,  $U$  and  $V$  by  $Q_h = Uhd$  and  $Q_v = Vld$ . In each compartment, we balance fluxes in and out, and obtain the following equations.

$$Q_h(S_i - S_{i-1}) = \kappa_1(S_i - C_{i-1}), \quad Q_v(C_i - C_{i-1}) = \kappa_1(S_i - C_{i-1}), \quad \text{for } i = 1 \dots N \quad (1)$$

where  $\kappa_1$  is the transfer coefficient, measured in m<sup>3</sup>/hr, of sucrose from the shredded cane to the juice. Here  $Q_h$  is known (because we know the conveyor belt speed  $U$ ), and  $Q_v$  can be estimated from the porous media flow (which has  $V \approx \rho g k / \mu \sim 0.15$  m<sup>3</sup>/m<sup>2</sup> min, assuming constant permeability  $k$  and viscosity  $\mu$ ). Two boundary conditions are required to uniquely determine the solution of (1). The megasse enters the diffuser with known concentration,  $S^*$ , of sucrose.

At the other end of the device (that is, the part of the device off the right hand end of the diagram shown in Figure 5), the megasse is compressed through two sets of rollers. Entering the rollers is 85 tonnes/hr of bound water and 50 tonnes/hr of free water. The bound water is associated with the sugar content  $S$  and the free water is associated with the sugar content  $C$ . After the rollers, the megasse simply contains 15 tonnes/hr of bound water, and the remaining water expelled from the

<sup>1</sup>Although shown as squares, these compartments are in fact parallelograms in the bed beneath each of the input jets due to the motion of the megasse (for a coordinate system fixed in space).

megasse is mixed with 50 tonnes/hr of fresh water and reintroduced into the system. We can see that there are several possible boundary conditions that can be imposed: here we give two such possibilities.

If we assume that the sugar in the free water entering the rollers has concentration  $C_1$ , then the relationship for  $C_0$  reads

$$C_0 = \frac{70}{170}S_0 + \frac{50}{170}C_1 = \lambda_1 S_0 + \lambda_2 C_1. \quad (2)$$

However, it is more likely that the sugar in the free water has some combination of  $C_0$  and  $C_1$ . At the other extreme, if the concentration of sugar in the water entering the rollers is  $C_0$ , we have

$$C_0 = \frac{70}{120}S_0 = \lambda_3 S_0. \quad (3)$$

Clearly the conditions at this end warrant further study. For now, we will assume that (3) holds. Thus we set

$$S_N = S^*, \quad C_0 = \lambda S_0. \quad (4)$$

The solution of (1) and (4) is

$$\frac{C_i}{S^*} = \frac{1 - \frac{M\lambda}{P} - (1 - \lambda) \left(\frac{1-P}{1-M}\right)^i}{1 - \frac{M\lambda}{P} - (1 - \lambda) \frac{M}{P} \left(\frac{1-P}{1-M}\right)^N}, \quad \frac{S_i}{S^*} = \frac{1 - \frac{M\lambda}{P} - \frac{M(1-\lambda)}{P} \left(\frac{1-P}{1-M}\right)^i}{1 - \frac{M\lambda}{P} - (1 - \lambda) \frac{M}{P} \left(\frac{1-P}{1-M}\right)^N}, \quad (5)$$

where  $M = \kappa_1/Q_h$  and  $P = \kappa_1/Q_v$ . We note that the ‘‘shape’’ of the solution changes depending on whether  $M$  or  $P$  is larger. If  $P > M$  (and both  $M$  and  $P$  are small), then the solution is of the form

$$C_i \sim A_1 + B_1 i - D_1 i^2, \quad (6)$$

where  $A_1$ ,  $B_1$  and  $D_1$  are all positive while if  $M > P$ , the third term in (6) changes sign. Thus we expect  $C_i$  to increase linearly with  $i$ , but to be concave or convex, depending on the relative sizes of  $M$  and  $P$ . In particular, we expect the solution to be concave when  $M > P$ , as shown in Figure 6.

The concentration of sucrose collected from the 13 trays in a test device is known, and shown as red dots in Figure 6. (We have localised all the tray data into one point, located at the start of the compartment). The solution to our model is fitted to these data (using the eyeball norm), and is shown as black dots in Figure 6. The agreement is excellent, but we note that we have allowed ourselves to choose  $\kappa$ ,  $Q_v$  and  $\lambda$ .

We note that the experimental parameters given are such that we would expect the solution to be convex, not concave, so we anticipate that the experimental results are from a different experiment from those yielding the standard data.

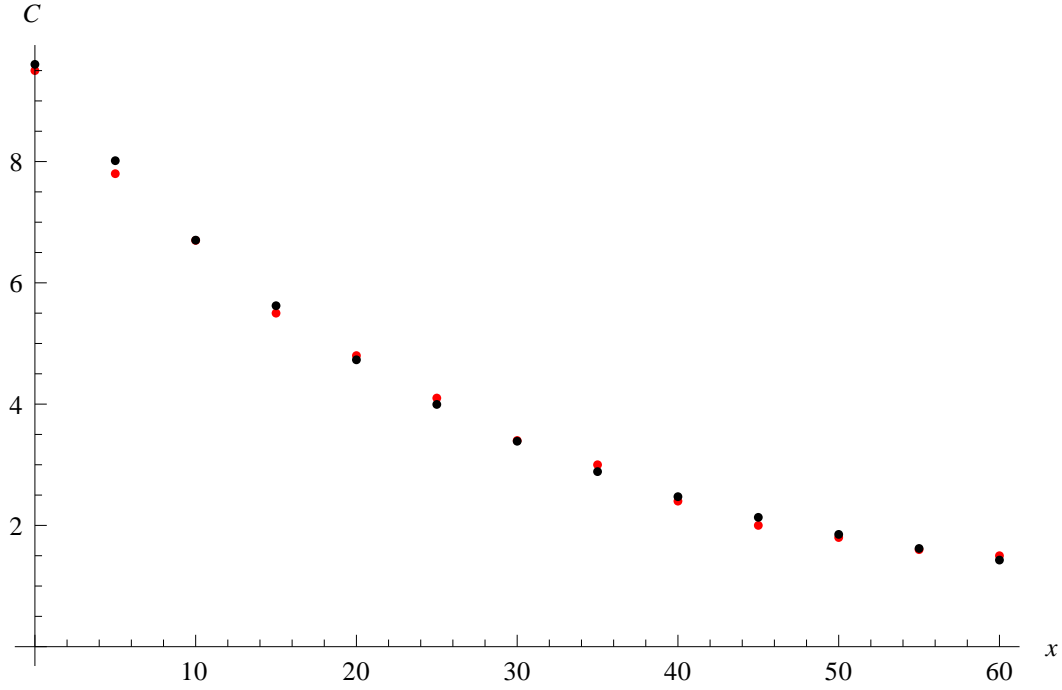


Figure 6: Graph showing experimental results (red dots) and the results of our discrete model (black dots). The (fitted) parameters are:  $M = 0.835$ ,  $P = 0.8$ ,  $\lambda = 0.975$ . The other parameters were  $N = 13$ ,  $S_0 = 10$ .

## 2.2 1-D continuum model

Since the number of stages in the diffuser is large, we take the continuum limit of the discrete model. We suppose that the start of the diffuser is located at  $x = 0$  and the end is at  $x = L$  and, remembering that  $x$  runs in the opposite direction to  $i$  in the discrete model, we end up with the following system:

$$-Q_v \frac{dC}{dx} = \kappa_2(S - C), \quad -Q_h \frac{dS}{dx} = \kappa_2(S - C), \quad (7)$$

where  $\kappa_2$  is the reaction rate, measured in  $\text{m}^2/\text{hr}$  ( $= hd\kappa_3$ , see later) with boundary conditions

$$S(0) = S^*, \quad C(L) = \lambda S(L). \quad (8)$$

We nondimensionalise the model using  $x = Lx'$ ,  $C = S^*C'$ , and  $S = S^*S'$ , yielding

$$C_x = -k_1(S - C), \quad S_x = -k_2(S - C), \quad (9)$$

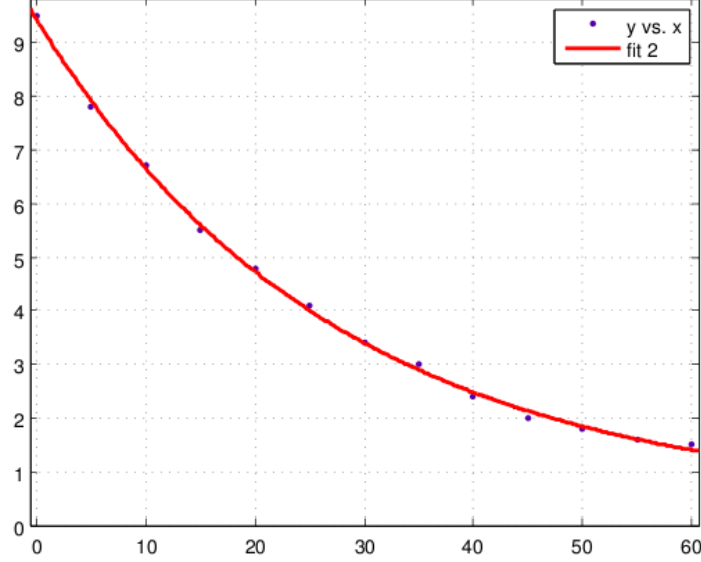


Figure 7: Graph showing (least squares) fit of the continuous model (in the form  $a + be^{-cx}$ ) to the data. The parameters were  $a = 2.98$ ,  $b = 0.72$ ,  $c = 0.42$ .

with

$$S(0) = 1, \quad C(1) = \lambda S(1), \quad (10)$$

where  $k_1 = \kappa_2 L / Q_v$ , and  $k_2 = \kappa_2 L / Q_h$ . The solution to (9) and (10) is:

$$C = \frac{(1 - \lambda\chi)e^{k_1(1-\chi)} - (1 - \lambda)e^{k_1(1-\chi)x}}{(1 - \lambda\chi)e^{k_1(1-\chi)} - (1 - \lambda)\chi}, \quad S = \frac{(1 - \lambda\chi)e^{k_1(1-\chi)} - (1 - \lambda)\chi e^{k_1(1-\chi)x}}{(1 - \lambda\chi)e^{k_1(1-\chi)} - (1 - \lambda)\chi}, \quad (11)$$

where  $\chi = k_2 / k_1$ . Again, the solution for  $C$  can be fitted using the data, as shown in Figure 7. We have again for simplicity assumed that each of  $\kappa$ ,  $\lambda$  and  $k_1$  can be chosen during the process.

The quantities of interest are the amount of sugar collected per hour (that is,  $Q_v S^* C(0)$ ) and the amount of sucrose leaving the diffuser in the shredded cane per hour ( $Q_h S^* S(1)$ ). Using the solutions in (11), we find the dimensional quantities are:

$$q_c = Q_v S^* C(0) = Q_v S^* \frac{(1 - \lambda \frac{Q_v}{Q_h}) e^{\frac{\kappa L}{Q_v} (1 - \frac{Q_v}{Q_h})} - (1 - \lambda)}{(1 - \lambda \frac{Q_v}{Q_h}) e^{\frac{\kappa L}{Q_v} (1 - \frac{Q_v}{Q_h})} - (1 - \lambda) \frac{Q_v}{Q_h}}, \quad (12)$$

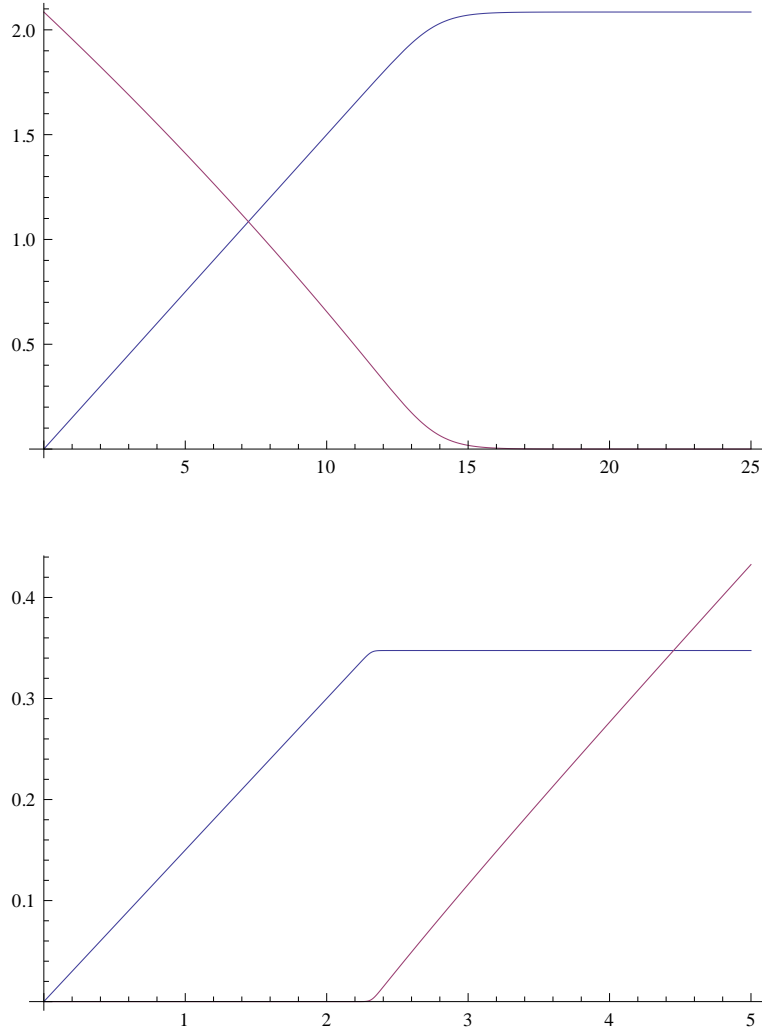


Figure 8: Upper graph shows how  $q_c$  (blue) and  $q_s$  (red) vary as  $Q_v$  varies ( $Q_h = 13.9$  tonnes/m<sup>2</sup>hr). Lower graph shows how  $q_c$  and  $q_s$  vary as  $Q_h$  varies ( $Q_v = 13.9/6$  tonnes/m<sup>2</sup>hr). Other parameters:  $S^* = 0.15$ ,  $L = 60\text{m}$ ,  $\kappa = 7.6$  tonnes/m<sup>3</sup>hr.

$$q_s = Q_h S^* S(1) = Q_h S^* \frac{1 - \frac{Q_v}{Q_h}}{(1 - \lambda \frac{Q_v}{Q_h}) - (1 - \lambda) \frac{Q_v}{Q_h} e^{-\frac{\kappa L}{Q_v} (1 - \frac{Q_v}{Q_h})}}. \quad (13)$$

We plot the solutions given in (12) and (13) in Figure 8.

We see that (see Figure 8(upper)) that increasing the flux of water through the system increases the amount of sugar recovered per hour, and decreases the sugar leaving the diffuser still in the megasse, while (see Figure 8(lower)) shows that, above a certain  $Q_h$ , the amount of sugar recovered does not change.

### 2.3 Extension to a 2-D model

In this section we write down the two-dimensional version of the continuous model. We let  $z$  be the vertical direction, with  $z = 0$  corresponding to the top surface of the megasse. Our 2-D model reads:

$$US_x = -\kappa_3(S - C), \quad UC_x + VC_z = \kappa_3(S - C), \quad (14)$$

where here the reaction rate  $\kappa_3$  has units  $\text{hr}^{-1}$ . The boundary conditions are

$$S(0, z) = S^*, \quad (15)$$

$$C(x, 0) = \lambda_1 \int_0^h S(L, z) dz + \lambda_2 \int_0^h C(L, z) dz, \quad \text{for } x = [L - l, L], \quad (16)$$

$$C(x, 0) = \frac{1}{l} \int_{nl}^{(n+1)l} C(x + h \frac{U}{V} + l, h) dx \quad \text{for } x = [nl, (n+1)L], n = 0..n-1. \quad (17)$$

As an illustration, we take a megasse which is 1 unit high and 30 units long. Plots of  $S$  and  $C$  are shown in Figure 9. We see that the concentration of sugar in the juice increases along the diffuser, and that the concentration of sugar bound in the megasse decreases both with depth through the megasse, and along the megasse.

## 3 Flow in the porous medium and tracer experiments

We now examine how the juice flows through the megasse from the injection points. We consider a simple model here in the main body of the text and examine a more complex and mathematically interesting problem in the Appendix. For the simple model we assume that the juice is sprayed at a sufficient rate to ensure that the megasse is saturated and that there is sufficient flooding of the top surface that the

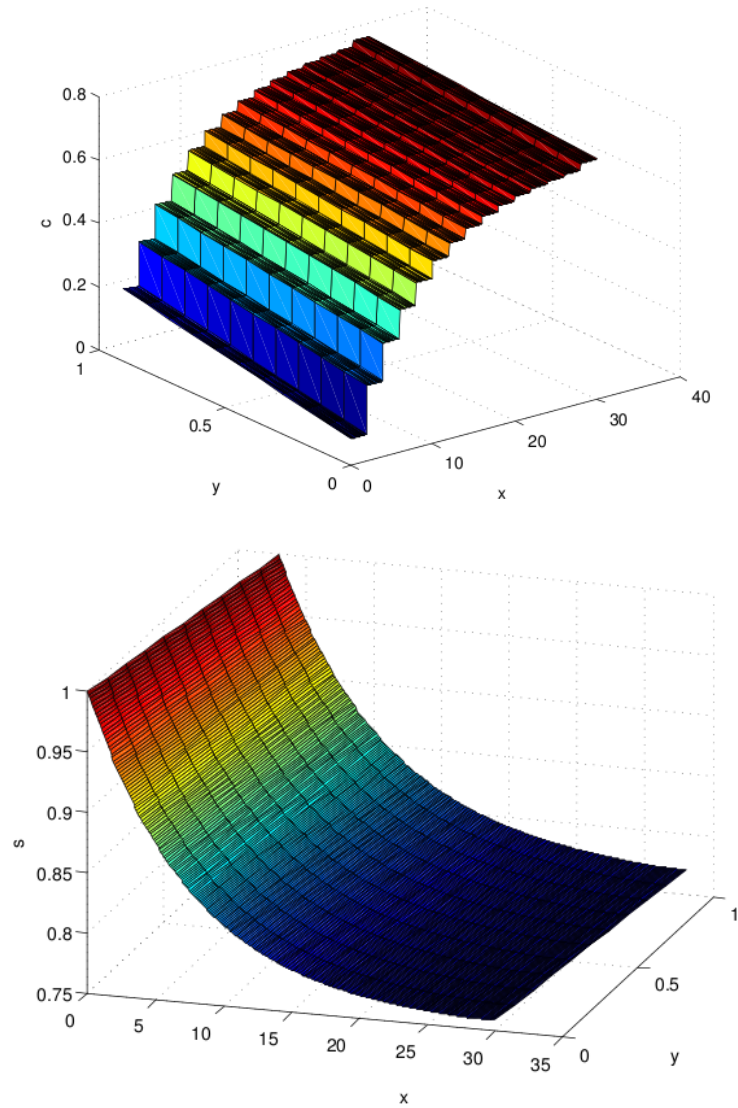


Figure 9: Graphs showing how  $C$  and  $S$  vary with position  $x$  along the diffuser and position  $y$  beneath the surface of the megasse. The parameters used were:  $\lambda_1 = 0.5$ ,  $\lambda_2 = 0.5$ ,  $U = 3$ ,  $V = 1$ ,  $\kappa_3 = 0.1$ ,  $h = 1$ ,  $L = 30$ , with 15 collection bins. Here  $y = z$ .

resulting flow is one-dimensional. The more complicated problem of determining the saturated flow from a finite size source and furthermore finding the flow from a finite source with an unsaturated surrounding region are presented in the Appendix.

For the simple case we shall account for the fact that the megasse may have some vertical structure and particularly that the permeability may vary with depth. This will allow us to examine possible void behaviour later in the text. Consider the problem of saturated flow in a region where the permeability varies with depth in the megasse. We assume that the flow is governed by D'Arcy's law and that the fluid is incompressible. Thus

$$\mathbf{u} = -\frac{\mathbf{k}(z)}{\mu} \nabla(p + \rho g z), \quad \nabla \cdot \mathbf{u} = 0, \quad (18)$$

where  $k(z)$  is the permeability,  $p$  is the pressure,  $\rho$  is the water density and  $\mu$  is the viscosity. We are interested in solving this equation across the megasse, which as before has thickness  $h$ . At the boundaries, we presume that the top ( $z = h$ ) is kept flooded with a thin layer of juice and that the bottom ( $z = 0$ ) is simply open, so that the pressure is atmospheric at both surfaces and hence

$$p = 0, \quad \text{on} \quad z = 0, h. \quad (19)$$

We note that there is no applied dependence on  $x$  and so the governing equation becomes

$$k p_{zz} + k' p_z + \rho g k' = 0, \quad (20)$$

which we can integrate to give

$$k p_z + \rho g k = \text{constant} = \mu V, \quad (21)$$

where  $V$  can be interpreted as the magnitude of the velocity. We can rearrange (21) and integrate to give

$$p = \int \left( \frac{\mu V}{k(\eta)} - \rho g \right) d\eta. \quad (22)$$

Imposing the two boundary conditions in (19), we then find

$$\int_0^h \frac{\mu V}{k(\eta)} d\eta = \rho g h, \quad (23)$$

which can be rearranged to give

$$V = \frac{\rho g h}{\mu \int_0^h \frac{d\eta}{k(\eta)}} = \frac{\rho g}{\mu \langle 1/k \rangle}, \quad (24)$$

where  $\langle . \rangle$  indicates an average value over the depth. We note that the fluid velocity is constant.

When the tracer is added, the concentration of the tracer,  $C$ , will be transported by convection and diffusion so that, relative to the megasse,  $C$  satisfies

$$C_t - VC_z = D_{\perp}C_{xx} + D_{\parallel}C_{zz}. \quad (25)$$

Here we have assumed that the flow within the porous media gives rise to anisotropic diffusivity (see Booth [1]). The two diffusivities, in the direction of the flow  $D_{\parallel}$  and perpendicular to the flow  $D_{\perp}$  can be well represented by

$$D_{\perp} = \frac{3}{16}VL, \quad D_{\parallel} = \frac{VL}{3} \log \left( \frac{3VL}{2D_m} \right), \quad (26)$$

where  $L$  is the average pore size (which is around 1mm) and  $D_m$  is the diffusivity of the tracer in the juice. This model is valid where  $VL/D_m$ , the pore-based Peclet number is sufficiently large, as is relevant for transport through the megasse.

We suppose that we inject a bolus of tracer at  $x = 0$  on the top surface at  $t = 0$ , that is, we have a point source at  $x = 0$ ,  $z = h$ , and that the transport is governed by (25). We thus have that

$$C = \delta(x), \quad \text{on} \quad z = h. \quad (27)$$

The solution is

$$C = \frac{Q}{t} \exp \left( -\frac{1}{4t} \left[ \frac{x^2}{D_{\perp}} + \frac{(z-h+Vt)^2}{D_{\parallel}} \right] \right), \quad (28)$$

where  $Q$  is determined by considering the size of the bolus.

We are interested in determining how the tracer spreads and exits from the megasse. This can be computed directly from (28), but it is instructive to consider the case where we can linearise the exponential and gain some insight. We thus approximate (28) by

$$C = \begin{cases} \frac{Q}{t} \left( 1 - \left( \frac{1}{4t} \left[ \frac{x^2}{D_{\perp}} + \frac{(z-h+Vt)^2}{D_{\parallel}} \right] \right) \right) & \text{when} \quad \frac{x^2}{D_{\perp}} + \frac{(z-h+Vt)^2}{D_{\parallel}} \leq 4t \\ 0 & \text{otherwise.} \end{cases} \quad (29)$$

Hence, at the bottom of the megasse,  $z = 0$ , we have

$$C = \begin{cases} \frac{Q}{t} \left( 1 - \left( \frac{1}{4t} \left[ \frac{x^2}{D_{\perp}} + \frac{(-h+Vt)^2}{D_{\parallel}} \right] \right) \right) & \text{when} \quad \frac{x^2}{D_{\perp}} + \frac{(-h+Vt)^2}{D_{\parallel}} \leq 4t \\ 0 & \text{otherwise.} \end{cases} \quad (30)$$

We use an illustrative set of parameters and show in Figure 10 the curve in the  $(x, t)$  plane where  $C$ , given by (30), transitions from zero to a positive value. We

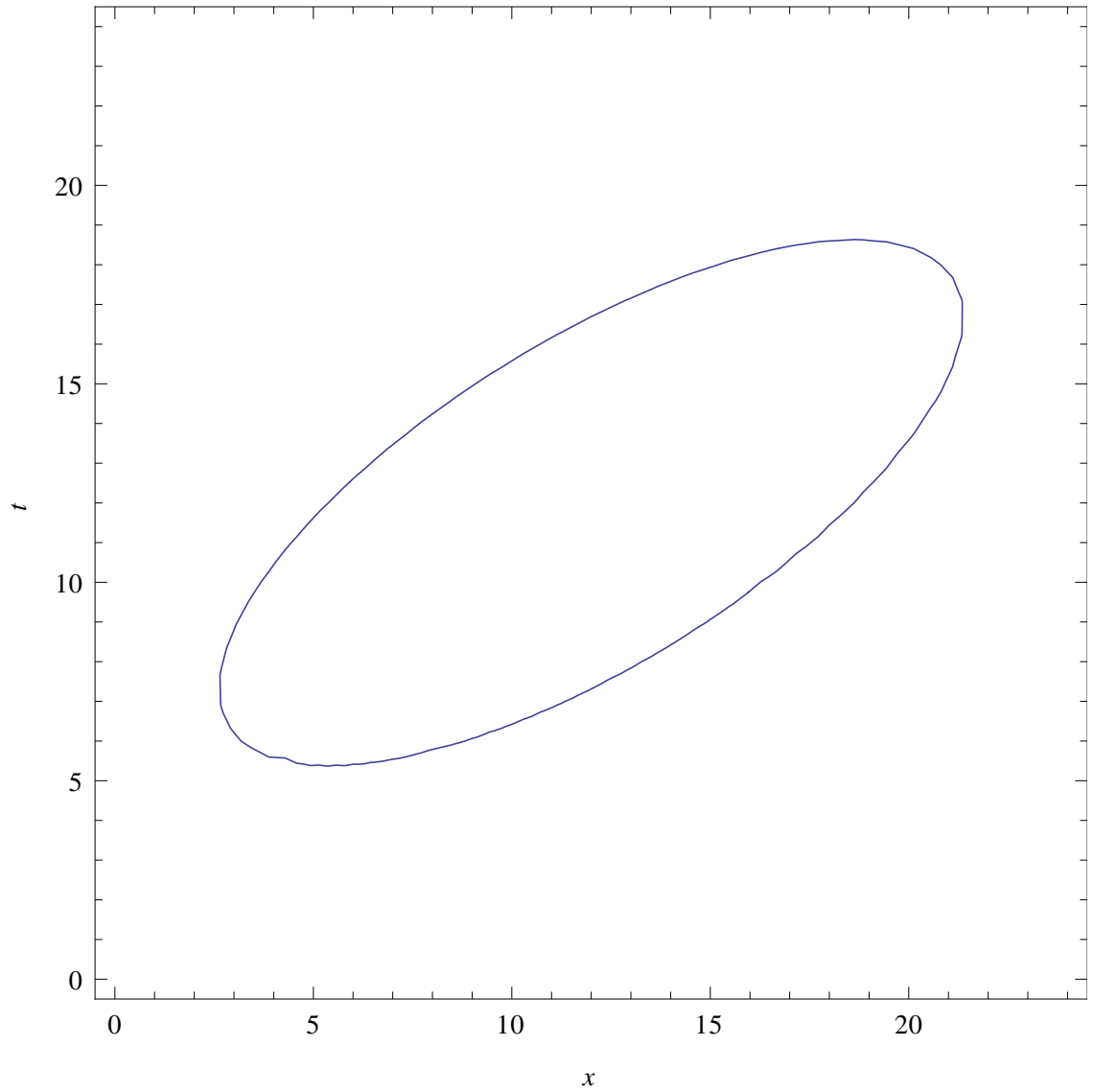


Figure 10: Plot of ellipse showing region of non-zero  $C$ . The parameters are  $D_{\perp} = 1$ ,  $D_{\parallel} = 0.01$ ,  $U = 1$ ,  $V = 0.1$ ,  $h = 1$ .

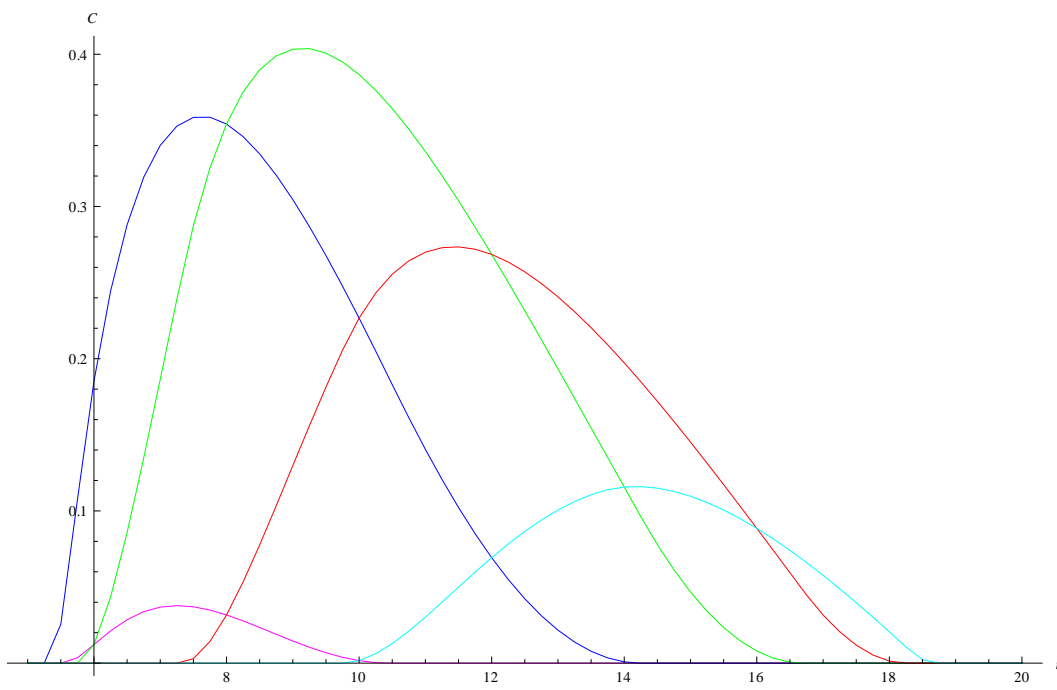


Figure 11: Average concentration in each bin as a function of time in five bins, each of width 4. Other parameters are as in Figure 10.

see that the region of nonzero  $C$  is enclosed in an ellipse with the minimum in time to the right of the minimum in space, which is true for an angled ellipse. Crucially, the ellipse is assumed to be much wider than the collector spacing and so we expect the juice containing the tracer to be collected in more than one box. Further, we see that, if the spacial separation between the two minima is greater than the collector spacing, or if the collector junction is between the two minima, then the juice will arrive in the downstream box before the upstream box. We illustrate this behaviour by assuming that the collectors are spaced 4 units apart, and we show the output of our simulated tracer experiment in Figure 11

Comparing the curves in Figure 11 with those in Figure 2, we see that both the relative sizes and timing of the collection of the juice is reproduced and thus we believe that our model explains this phenomena.

We note that our parameter choices were made in order to create solutions with the observed behaviour. We have yet to reconcile these with the physical parameters and, in particular, note that if we use more physically realistic numbers then the aspect ratio of the ellipse (in Figure 10) decreases dramatically and the initial arrival time of the juice in the bins travels downstream at a constant rate (unlike Figure 11).

## 4 Simple model for voids

In this section we consider one possible mechanism for the formation and influence of voids in the megasse which, as noted earlier, are undesirable. These voids are regions of the megasse where it appears that there is little or no water, as illustrated in Figure (12).

The possible mechanism is one of cavitation. To avoid cavitation, we anticipate that the pressure in the juice must not drop below atmospheric (zero) pressure. We

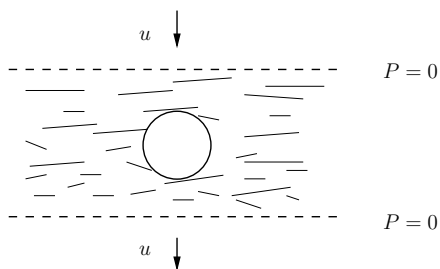


Figure 12: Schematic of a void within the megasse.

expect that, if the megasse has uniform microscopic structure, then the pressure everywhere is identically atmospheric. Hence, we briefly explore here how the pressure depends on nonuniformity within the megasse and identify regions of negative pressure as places where cavitation and hence voids can occur.

These regions where the the pressure is negative (less than atmospheric) are ripe for any stray air bubbles to coalesce, and form a stable cavity. This model does not describe other factors such as surface tension and geometric structure, however, it does highlight unwanted pressure zones. We will therefore not examine what the flow through the megasse is when cavitation occurs but only indicate when it might be observed.

Our starting assumption is again that the flow is one dimensional, and governed by D'Arcy's law as outlined and solved in Section 3. The flow was found to have a velocity

$$V = \frac{\rho g h}{\mu \int_0^h \frac{d\eta}{k(\eta)}} \quad (31)$$

with the pressure being given by

$$p = \rho g h \left( \frac{\int_0^y \frac{d\eta}{k(\eta)}}{\int_0^h \frac{d\eta}{k(\eta)}} - \frac{z}{h} \right). \quad (32)$$

In practice, the fines within the megasse tend to move towards the bottom where the megasse is more compressed and hence we expect the permeability to decrease as we approach  $y = 0$  (the permeability would be monotonically increasing with  $y$ ). Since the pressure gradient is given by

$$\frac{dp}{dz} = \rho g h \left( \frac{1}{k(z) \int_0^h \frac{d\eta}{k(\eta)}} - \frac{1}{h} \right). \quad (33)$$

we note that, if  $k(z)$  is monotonic increasing, then  $dp/dz$  can only be zero at one point. Hence we conclude that if the permeability decreases monotonically with its minimum at the bottom, the pressure is everywhere greater or equal to zero so no voids appear, while the converse occurs if the permeability increases monotonically.

Some numerical experiments were performed with various piecewise constant permeabilities, and the pressure determined, as shown in Figures 13 and 14. From this we conclude that if there are regions of low permeability above regions of high permeability, there is the possibility of cavitation. However, the natural tendency for the low permeability regions to be at the bottom of the megasse are likely to mitigate against this behaviour. We note that if mechanical devices, such as rotating

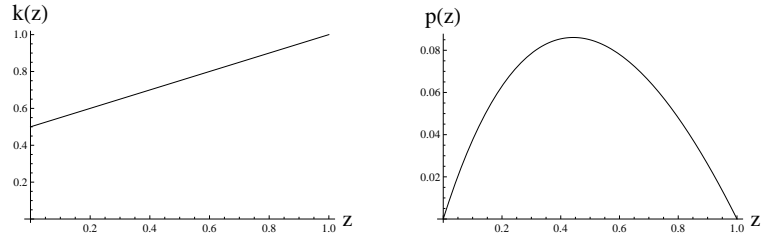


Figure 13: The left graph shows nondimensional permeability and the right graph the resulting nondimensional pressure distribution in the case of linearly increasing permeability towards the bottom of the megasse with no resulting cavitation.

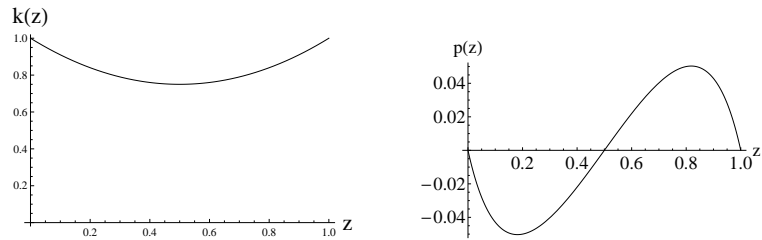
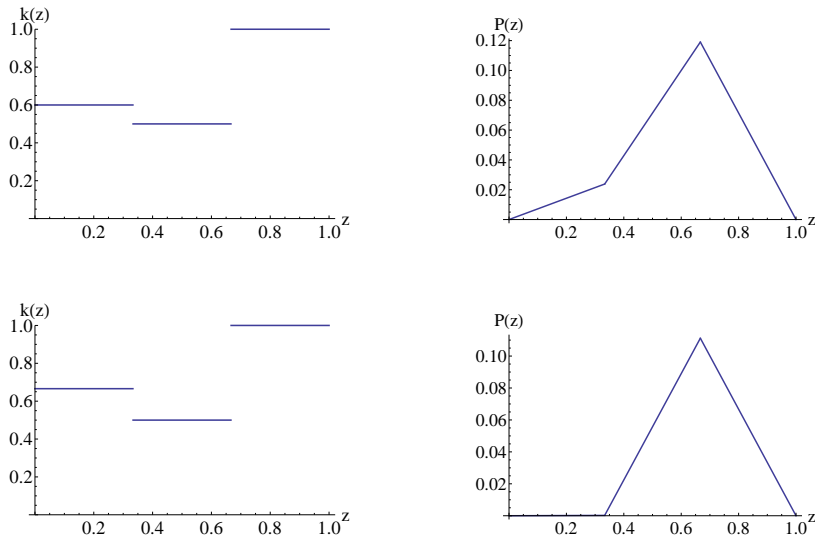


Figure 14: The left graph shows nondimensional permeability and the right graph the resulting nondimensional pressure distribution in the case of quadratically varying permeability of the megasse with cavitation possible.



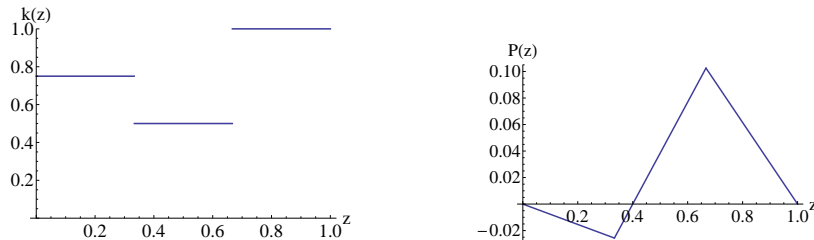


Figure 15: The left graph shows the piecewise linear nondimensional permeability and the right graph the resulting nondimensional pressure distribution.

screws, are present at some intermediate point in the diffuser to mix the megasse, this will enhance the possibility that voids will form subsequently.

To illustrate that the possibility of cavitation depends on the permeability variation through the entire megasse bed, and is not purely a locally determined phenomenon, we consider some piecewise linear permeability distributions. These are given in Figure 15 and show that for similar variations of the permeability cavitation is sensitive to the relative size of the permeability in all the regions. It is worth noting that when cavitation does occur it tends to be in regions where the permeability of the region immediately above is higher. Note that this would indicate that including a relative low permeability layer under the megasse would reduce the opportunity for cavitation but would reduce the resulting flow rate.

## 5 Conclusions

In this report we have presented discrete and continuous mathematical models for the flow of sugar cane and juice through a sugar diffuser, with the aim of describing how the amount of dissolved sugar in the juice increases during this industrial process. Our simple discrete and continuous models were able to capture qualitatively the concentration in the juice. We also extended these simple models to two dimensions.

We considered the flow through the megasse and determined that the fluid moved downwards with constant velocity. We then considered the injection of a tracer at one of the jets on the surface. Our model included different diffusivities for the tracer in the “with the flow” and “across the flow” directions. We solved the model using a simple approximation, and found that with a set of test parameters we were able to reproduce the behaviour that is seen in the tracer experiments.

We have examined a simple cavitation mechanism for creating dry regions in voids in the megasse. We have shown that they may occur when the permeability varies in such a way as to produce regions of possible negative pressure. The ex-

istence of such regions depends on the permeability variations through the entire depth of the bed but is exacerbated by regions of low permeability away from the bottom of the bed.

All our models contain parameters which need to be obtained from experiments: the next stage would be to use these to give our models real predictive power.

## References

- [1] R. Booth, Miscible flow through porous media, DPhil Thesis, Oxford University, 2008.
- [2] Bear, J. Dynamics of Fluids in Porous Media, McGraw Hill, 1972.
- [3] Harr, M. Groundwater and Seepage, McGraw Hill, 1962.
- [4] Zhukovsky, N. "Collected Works" Gostekhizdat, Moscow, 1949-1950.

## Appendix

### Flow through megasse due to applied pressure

In this appendix we consider the problem of porous media flow through the megasse in the situation where the top surface has a region of excess pressure. In this case, we consider how water spreads and flows downward through a previously dry section of megasse. As a result, there is a region of fully saturated flow surrounded by a dry region. In what follows we consider the flow downward from a single source and then extend this to the case of multiple sources.

#### A.1 Equations

The flow of a liquid through a porous medium can be studied by defining the piezometric head

$$\Phi = \frac{\hat{p}}{\rho g} + Y, \quad (34)$$

where  $Y$  is elevation,  $\hat{p}$  is the pressure,  $\rho$  is density and  $g$  is gravitational acceleration. The usual model assumes the flow is dictated by Darcy's Law, which states that the fluid velocity  $\hat{\mathbf{u}}$  is given as

$$\hat{\mathbf{u}} = -\kappa \nabla \Phi, \quad (35)$$

where  $\kappa = \rho g k / \mu$ ,  $k$  is permeability of the material and  $\mu$  is dynamic viscosity of the fluid. Combining Darcy's Law with the continuity equation gives

$$\nabla \cdot \hat{\mathbf{u}} = -\kappa \nabla^2 \Phi = 0 \quad (36)$$

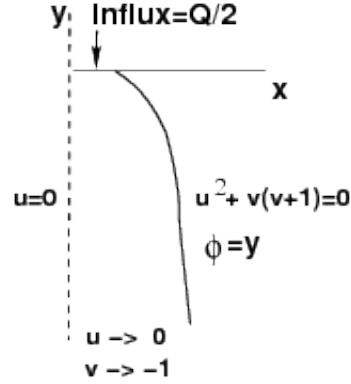


Figure 16: Flow of downward plume with narrow inflow source.

or Laplace's equation for the piezometric head. If there are any air-water boundaries present, then they should satisfy the condition that pressure  $\hat{p} = 0$  so that  $\Phi = Y$  on that surface.

It is convenient to non-dimensionalize with respect to a length scale  $H$ , a velocity scale  $\kappa$  and a pressure scale  $\rho g H$ . In that case,  $\phi = \Phi/H$ ,  $y = Y/H$ ,  $p = \hat{p}/(\rho g H)$ , and  $\mathbf{u} = \hat{\mathbf{u}}/\kappa$  and the resulting equations become

$$\nabla^2 \phi = 0, \quad (37)$$

where  $\mathbf{u} = -\nabla \phi$  and  $\phi = y$  on the free surface.

An alternative equation for the free boundary condition can be obtained by noting that  $\mathbf{u} \cdot \mathbf{n} = 0$  where  $\mathbf{n}$  is a normal to the surface so that  $\mathbf{u} \cdot \nabla(\phi - y) = 0$ , giving the condition

$$u^2 + v(v + 1) = 0. \quad (38)$$

## A.2 A single plume flow

To begin, it is of interest to examine the spread of the water flowing downward through a porous medium in a two-dimensional plume with a source at the surface. Assuming the belt is not moving, we can analyse the problem shown in Figure 16 with an inflow at the top and free boundaries on the sides. Since the flow is symmetric we only consider the right side of the flow region.

Equation (38) gives a condition that as the liquid drains through the sugar pulp, it will eventually become a vertical flow, so that  $u \rightarrow 0$ , which means that  $v \rightarrow -1$ . As a result, we can say that if the input flux at the top is  $Q/2$ , then the limiting half-width of the plume is  $W = Q/2$ . Note that this is independent of the width

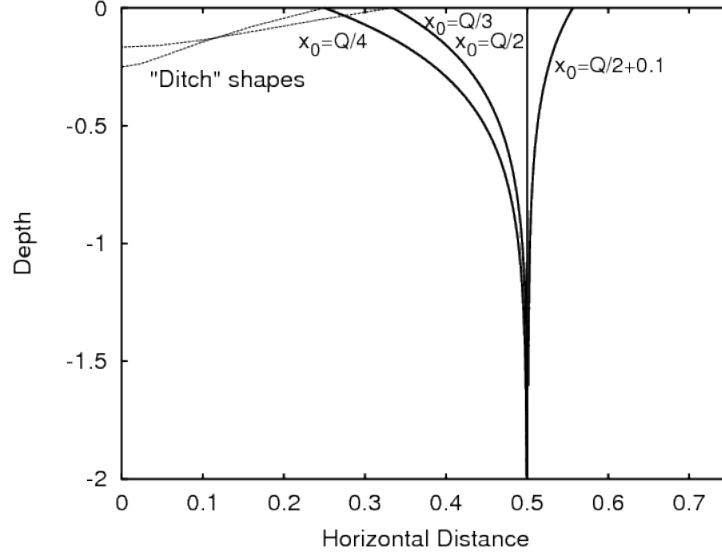


Figure 17: Solutions for flows with initial flux of  $Q = 1$  and initial plume half-widths of  $Q/4, Q/3, Q/2$  and  $Q/2 + 0.1$ . All surfaces become vertical exponentially.

over which the liquid is drained onto the surface. The question then is how quickly is this thickness reached?

A neat method to consider this flow is to use the Zhukovsky function, [3, 4] which is defined as

$$\theta = iz + f = Ae^{-f/\alpha} \quad (39)$$

where  $f = \phi + i\psi$  is a complex potential,  $z = x + iy$  are the coordinates in the physical plane and  $\alpha$  and  $A$  are constants to be determined. The velocity components are related to the complex potential via the relations  $u = -\phi_x$  and  $v = -\phi_y$ . This function is analytic and hence satisfies Laplace's equation. The method will provide a solution for seeping flow from a ditch of some width and depth. The shape of the ditch is not known a-priori, but in this problem is not particularly relevant since our interest is in the behaviour of the free surface. More detailed explanation of this can be found in [3].

Taking real and imaginary parts in equation (39) we find that in general

$$x = -\psi - Ae^{-\phi/\alpha} \sin \frac{\psi}{\alpha}, \quad (40)$$

$$y = \phi - Ae^{-\phi/\alpha} \cos \frac{\psi}{\alpha}. \quad (41)$$

We note that on the line of symmetry  $x = 0$ ,  $\psi = 0$  and on the free surface  $\psi = -Q/2$  and also  $\phi = y$ . Therefore on the surface it must be that either  $A = 0$  or

$\cos \psi/\alpha = 0$ , that is,  $\psi/\alpha = (2n + 1)\pi/2$  and so  $\alpha = -Q/(2n + 1)/\pi$ . It turns out that the appropriate choice of  $n$  is  $n = 0$ , (for other choices see [3]) in which case we have  $\alpha = -Q/\pi$  and using  $y = \phi$  gives

$$x = \frac{Q}{2} - Ae^{\pi y/Q}. \quad (42)$$

As expected, the width of the plume approaches  $Q/2$  as  $y \rightarrow -\infty$ . Noting that at  $y = 0$ ,  $x = x_0$ , the initial half-width of the inflow region, we obtain  $A = Q/2 - x_0$ . It is clear from this result that convergence to the final plume thickness occurs very quickly (exponentially in fact). It is of interest to compute the shape of the drainage ‘‘ditch’’, although it is only of minor concern and not relevant to our conclusions. On the surface of the ditch,  $\phi = 0$ , and so we can use equation (40) with  $\phi = 0$  over  $-Q/2 < \psi < 0$  to find that

$$x_D = -\psi - (Q/2 - x_0) \sin\left(\frac{\psi\pi}{-Q}\right), \quad (43)$$

$$y_D = (x_0 - Q/2) \cos\left(\frac{\psi\pi}{Q}\right). \quad (44)$$

Some examples of surface shapes are given in Figure 17. The dashed lines indicate the shape of the ‘‘ditches’’ for  $x_0 = Q/4$  and  $x_0 = Q/3$ . The case  $x_0 = Q/2$  is an exact solution with  $x = Q/2$  everywhere (the inflow region is exactly the same as the final plume width) with a flat seepage zone through the top. The case  $x_0 = Q/2 + 0.1$  is simply an example to show that even if the inflow region is slightly wider than the final plume width, the plume narrows to the limiting thickness. In this case the ‘‘ditch’’ is actually a small mound (not shown).

The main point of this work is to show that for reasonable inflow widths across the top of the sugar pulp the transition to the final plume thickness is exponentially fast, meaning we can assume that the flow is close to uniform as it exits from the bottom of the pulp layer. It is also important to note that the limiting dimensional velocity through the bottom is given by the magnitude of the hydraulic conductivity, that is,  $\bar{v} \rightarrow -\kappa$ .

### A.3 Saturated solution

The above work seems to suggest that the flow reaches its full width very quickly (exponentially in fact) and so if the flow is large enough to fill each section between inflow points then we can assume the region is fully saturated. It is also reasonable to assume that the flow is periodic in the x-direction (before the horizontal motion is included). The results above suggest that the flux from the base will be close to uniform, which will allow us to specify the flow fully in terms of the inflow.

The equations describing a saturated flow of this kind are, similar to above, Laplace's equation for the piezometric head and periodicity in the  $x$  direction. In non-dimensional coordinates we define  $y = 0$  to be the bottom and  $y = 1$  to be the top of the layer. On the top surface we can specify the inflow to be a step-function

$$\phi_y = \begin{cases} 0 & -L < x < -\beta/2 \\ -V_0 & -\beta/2 < x < \beta/2 \\ 0 & \beta/2 < x < L \end{cases} \quad \text{on } y = H$$

where  $2L$  is the distance between inflow sources and  $\beta$  is the width of the source of water. We could specify any inflow function, but this seems to closely approximate the current situation. We assume the water is injected directly into the surface. On the bottom we can specify the flux so that

$$\phi_y = -V_B, \quad \text{on } y = 0, \quad -L < x < L, \quad (45)$$

where  $V_0\beta = 2V_B L$  by conservation. It is possible to account for some of these conditions by choosing  $\phi$  carefully. Using separation of variables we can write

$$\phi(x, y) = -V_B y - cx + \sum_{k=0}^{\infty} a_k \cosh \lambda_k y \cos \lambda_k x \quad (46)$$

where  $\lambda_k = 2k\pi/L$ . Thus we note that this form satisfies the conditions at  $y = 0$  and  $x = \pm L$ . It remains to satisfy the top surface condition at  $y = 1$ , for which we can invoke orthogonality of the eigenfunctions and obtain,

$$a_0 = \frac{V_0 L - 2\beta V_B}{L}, \quad (47)$$

$$a_k = \frac{-V_B L \sin \lambda_k \beta}{(k\pi)^2 \sinh \lambda_k}, \quad k = 1, 2, 3, \dots \quad (48)$$

In order to see the streamlines of the flow we can use the Cauchy-Reimann equations to find the streamfunction

$$\psi(x, y) = -cy + V_B L \sum_{k=1}^{\infty} \frac{\sin \lambda_k \beta}{(k\pi)^2 \sinh \lambda_k} \sinh \lambda_k y \sin \lambda_k x. \quad (49)$$

A solution for a segment length of  $2L = 4$ , height  $H = 1$  no horizontal movement is given in Figure 18. The streamlines indicate a rapid spread sideways and a vertical (reasonably parallel) downward finish.

The two figures show examples of the streamlines for the case in which the conveyor is not moving (Figure 18) and one which is moving to the right with speed

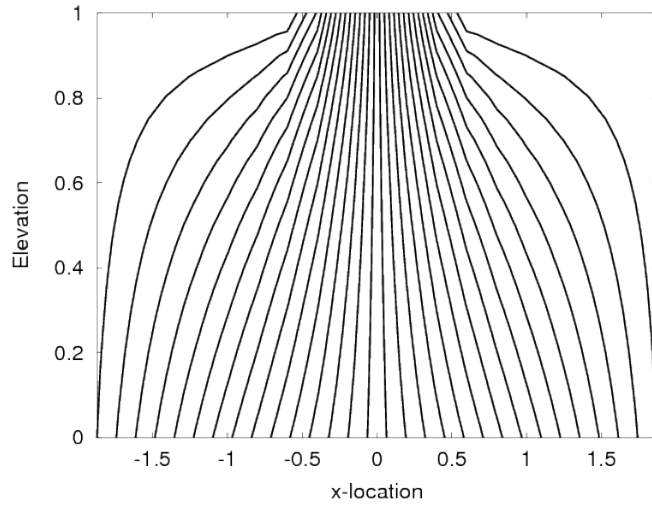


Figure 18: Streamlines for no horizontal motion, an inflow width of  $\beta = 0.5$ , segment length of 4 and height  $H = 1$ .

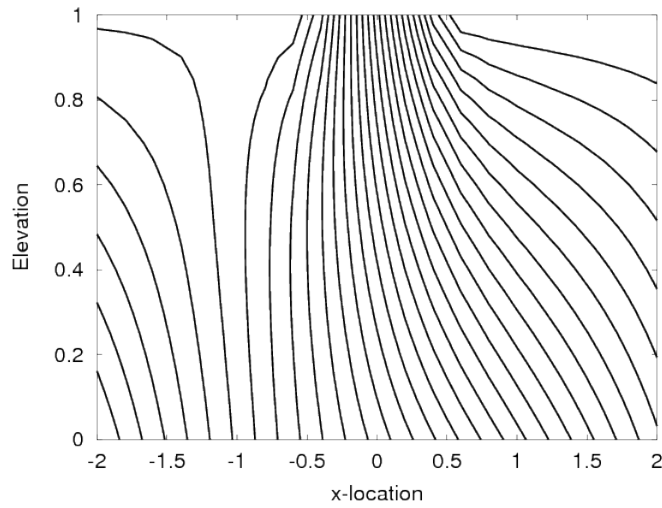


Figure 19: Streamlines for horizontal motion  $c = 0.02$ , an inflow width of  $\beta = 0.5$ , segment length of  $2L = 4$  and height  $H = 1$ .

$c = 0.02$ . The streamlines of these flows are steady, even though the conveyor is moving the sugar pulp along. The results indicate that there are dividing streamlines between each inflow section and according to this model the fluid from each inflow stays within those bounds. The water from each inflow source will then be more or less captured in a section of length  $2L$  downstream a distance of approximately  $D = cT = c\kappa/H$  from the inflow source, where  $c$  is the conveyor speed,  $2L$  is the distance between inflow points,  $\kappa$  is the hydraulic conductivity and  $H$  is the height of the sugar cane pulp layer.

#### **A.4 Comments**

The results above indicate that the water inflow will quickly spread to its final plume thickness and join up with the plume from the next inflow. The flow out through the bottom should then be fairly uniform. Assuming saturated flow, the liquid will pass through the layer remaining within the horizontal confines of each section (subject to horizontal translation).

This model does not take account of possible mixing at the dividing streamlines or the possibility of preferred pathways and nor does it allow for variable permeability near the base of the layer. It would seem likely, however, that these effects may not be great - altering the timing of the water's passage through the layer rather than the width of the section, since this is fixed by the process. A more complicated model could be invoked to consider this, but in effect an average permeability would seem to be adequate to capture the main behaviour.